Facilitation at single synapses probed with optical quantal analysis

Thomas G. Oertner, Bernardo L. Sabatini, Esther A. Nimchinsky and Karel Svoboda

Howard Hughes Medical Institute, Cold Spring Harbor Laboratory, 1 Bungtown Road, Cold Spring Harbor, New York 11724, USA
Correspondence should be addressed to K.S. (svoboda@cshl.edu)

Published online: 10 June 2002, doi:10.1038/nn867

Many synapses can change their strength rapidly in a use-dependent manner, but the mechanisms of such short-term plasticity remain unknown. To understand these mechanisms, measurements of neurotransmitter release at single synapses are required. We probed transmitter release by imaging transient increases in [Ca^{2+}] mediated by synaptic *N*-methyl-D-aspartate receptors (NMDARs) in individual dendritic spines of CA1 pyramidal neurons in rat brain slices, enabling quantal analysis at single synapses. We found that changes in release probability, produced by paired-pulse facilitation (PPF) or by manipulation of presynaptic adenosine receptors, were associated with changes in glutamate concentration in the synaptic cleft, indicating that single synapses can release a variable amount of glutamate per action potential. The relationship between release probability and response size is consistent with a binomial model of vesicle release with several (>5) independent release sites per active zone, suggesting that multivesicular release contributes to facilitation at these synapses.

Classic studies of the neuromuscular junction identify the vesicle as the quantum of synaptic transmission[1]. The neuromuscular junction contains many active zones, defined ultrastructurally as patches of membrane-associated material studded with docked synaptic vesicles. Each active zone releases vesicles independent of other active zones, and the amplitude distribution of postsynaptic potentials can be described quantitatively by a binomial model[1]. Most glutamatergic synapses of the CNS, such as those between hippocampal CA3 and CA1 pyramidal neurons (CA3–CA1 synapses), contain one active zone with several (2–20) docked vesicles, apposed to a single postsynaptic density[2,3]. In response to an action potential (AP), each synapse releases neurotransmitter with a characteristic probability, and considerable heterogeneity exists between synapses in their release properties[4,5]. If each docked vesicle were ready to fuse independently in response to an AP, then the simultaneous release of multiple quanta would occur on occasion. For example, if two docked vesicles each released with a probability of 0.5, then the simultaneous release of two vesicles would occur with a probability of 0.25. Although some studies have found evidence for multiquantal release[6–9], most experiments, using a variety of approaches, indicate that at most a single vesicle can be released in response to an AP[5,10–14]. This 'univesicular release rule' stipulates that one released vesicle would rapidly (within microseconds) inhibit the release of other docked vesicles within the same active zone[12]. Thus, determining if and under which conditions multivesicular release can occur has important implications for understanding the mechanisms of neurotransmitter release and synaptic plasticity.

Testing the univesicular release rule requires the technically difficult measurement of transmission at single synapses. One vesicle of neurotransmitter is thought to activate only a few postsynaptic receptors, producing small unitary currents[8,15,16]. Most synapses are located within an extensive dendritic tree and currents measured at the soma are highly filtered and attenuated[8,17–19]. In addition, it is difficult to ensure that one is recording from a single synapse using electrophysiological techniques alone[8,17]. To probe transmission at single synapses, we imaged NMDAR-mediated [Ca^{2+}] accumulations in individual spines[20] as a measure of glutamate release. Previous studies using serial section electron microscopy have shown that most spines participate in only one excitatory synapse[3,21]; therefore, NMDAR-mediated synaptic [Ca^{2+}] transients in single spines report release from single active zones. We found that the amount of glutamate released per action potential could be modulated with manipulations that change release probability. Our findings are quantitatively consistent with multivesicular release from multiple independent release sites at single active zones.

Results

To probe transmission at single synapses, we imaged [Ca^{2+}] accumulations in single spines produced by NMDAR currents[20] using two-photon laser scanning microscopy[22,23]. Synaptic NMDARs are far from saturated by glutamate release produced by a single AP[20,24,25] and NMDAR activation is a quantitative measure of glutamate in the synaptic cleft. To monitor glutamate release optically, it was necessary to isolate NMDAR-mediated Ca^{2+} currents, as Ca^{2+} influx into spines can occur through multiple pathways[26]. Recorded neurons were voltage-clamped slightly above NMDAR reversal potential (+10 mV), inactivating voltage-sensitive Ca^{2+} channels[20]. At these depolarized potentials, the Mg^{2+} block of NMDARs is relieved. AMPA (α-amino-3-hydroxy-5-methyl-4-isoxazole propionic acid)-type glutamate receptors were blocked by the AMPA receptor (AMPAR) antagonist NBQX (10 μM). The remaining synaptic

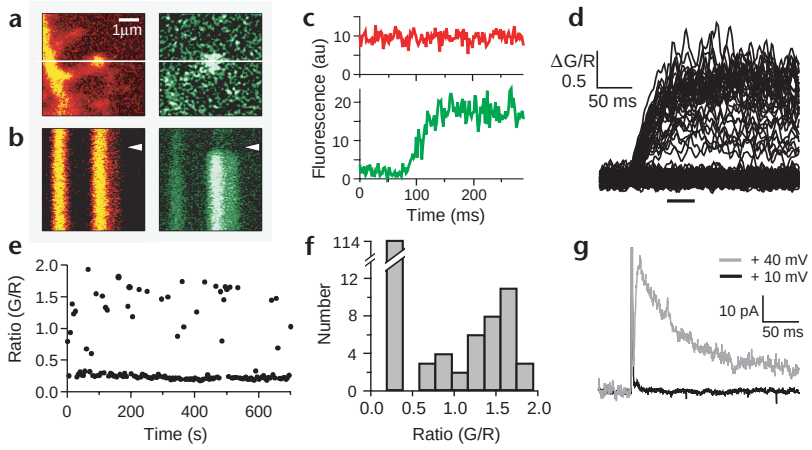

Fig. 1. Measurement of NMDAR-mediated $[Ca^{2+}]$ transients in single spines. (**a**) Left, dendrite with several spines (red fluorescence) and right, $[Ca^{2+}]$ transient after synaptic stimulation (green fluorescence, ΔG). White line indicates position of the line scan. (**b**) Line scans across spine head (total duration, 450 ms). White triangles indicate time of synaptic stimulation. Red fluorescence did not change (left), whereas green fluorescence increased rapidly in the spine after synaptic stimulation (right). A weak and delayed increase in $[Ca^{2+}]$ due to Ca^{2+} diffusion is apparent in the dendrite. (**c**) Time course of fluorescence intensity in the spine head in the $[Ca^{2+}]$-insensitive (red) and $[Ca^{2+}]$-sensitive (green) fluorescence channels (single trial, same data as in **b**). (**d**) Multiple responses to synaptic stimulation with single pulses (130 trials). Failures of neurotransmitter release can be clearly distinguished from successes. (**e**) Response amplitudes over time. Response amplitudes, failure rates, and resting fluorescence (corresponding to resting $[Ca^{2+}]_i$) were stable (same data as in **d**); response amplitudes were averaged in a 40 ms window starting 50 ms after stimulation (horizontal bar at bottom of **d**). (**f**) Histogram of response amplitudes. (**g**) EPSC measured in the soma at nominal holding potentials of +10 mV (black) and +40 mV (gray). The initial fast transient is the stimulus artifact.

$[Ca^{2+}]$ transients were completely blocked by antagonists of NMDARs (10 µM APV; 97 ± 1%, $n = 5$)[20]. We performed our quantitative imaging in line-scan mode[20,22,27], allowing detection of quantal fluorescence transients with a sufficient signal-to-noise ratio to clearly distinguish trials in which neurotransmitter was (successes) or was not (failures) released (**Fig. 1**). Synaptic responses could be monitored for 80–200 trials (**Fig. 1d** and **f**) and thus allowed the measurement of the probability of failure to release neurotransmitter at a single synapse. We define the probability of release (of one or more quanta) at a synapse in response to a single stimulus as P' = (1-failure probability). P' varied greatly across synapses (range, 0.18–0.62; mean, 0.33). The coefficient of variation (c.v.) of the response amplitudes (c.v. = s.d./mean, excluding failures; **Fig. 1f**) was 0.37 (range, 0.22–0.48), similar to the variability of miniature excitatory postsynaptic currents (EPSCs) in slices (c.v. = 0.42)[28].

Many types of synapses show a type of short-term plasticity called paired-pulse facilitation (PPF)[12,29]. When two APs invade presynaptic terminals in close succession (10–300 ms), the amount of transmitter released in response to the second AP is greater, on average, than to the first. PPF is usually measured for populations of synapses and can be quantified as PPF = EPSC(t_{ISI})/EPSC(0), where t_{ISI} is the interstimulus interval and EPSC(t) is the excitatory postsynaptic current measured at the soma following a stimulus at time t. Under our experimental conditions, PPF peaked somewhere between 10–20 ms and decreased with a decay time of ~200 ms. Similar time courses were measured for currents dominated by AMPARs (**Fig. 2a**) and NMDARs (**Fig. 2b** and **c**).

To analyze the mechanisms of facilitation, we imaged PPF of postsynaptic $[Ca^{2+}]$ transients at single synapses (PPF_{Ca}; **Fig. 3**). We distinguished between the average response amplitude (R), where the average was computed over all trials including failures (the usual measure of synaptic strength), and the average response potency[10] (r), where the average was computed over successes only (**Fig. 3c** and **d**). $PPF_{Ca} = R''/R'$, where R' and R'' are the average response amplitudes to the first and second pulse, respectively (**Fig. 3a**). The univesicular release rule implies that potency should not change during plasticity, and therefore PPF_{Ca} should be equal to the potentiation of release probabilities: $PPF_{Ca} = R''/R' = P''/P'$, where P' and P'' are the synaptic release probabilities to the first and second pulse (see Methods). Alternatively, facilitation could involve an increase in potency, consistent with multivesicular release. In this case, the ratio of synaptic release probabilities by itself would not account for the observed plasticity, and $PPF_{Ca} > P''/P'$.

In our measurements, it was possible to sort responses to a pair of stimuli into four categories corresponding to the four possible permutations of failures and successes for each stimulus (**Fig. 3c**). Each outcome has an associated probability (p_{ij}), where the subscript i indicates failure ($i = 0$) or success ($i = 1$) in response to the first stimulus and the subscript j indicates failure or success in response to the second stimulus ($p_{00} + p_{01} + p_{10} + p_{11} = 1$). We can compute synaptic release probabilities as $P'' = (p_{01} + p_{11})$ and $P' = (p_{10} + p_{11})$. For all synapses probed at $t_{ISI} = 100$ ms, $PPF_{Ca} > P''/P'$ ($P < 0.01$, $n = 8$), suggesting that PPF_{Ca} was in part due to increases in potency.

A direct measure of potency changes during PPF_{Ca} is given by comparing the potency of the first response (or the potency in response to a single stimulus, r) to the potency of the second response, given there was a failure on the first stimulus (r_{01}; **Fig. 3c**). In this comparison, we used facilitated responses that produced release only on the second stimulus so that we could exclude postsynaptic mechanisms of facilitation. The univesicular release rule predicts the potency ratio $(r_{01}/r)^* = 1$ (* denotes a model prediction). In the example of **Fig. 3**, $r_{01}/r = 1.77$ (**Fig. 3d** and **f**), which is inconsistent with the univesicular release rule. For every synapse measured with $t_{ISI} = 40$ ms, we found that r_{01}/r was significantly ($P < 0.05$) larger than 1 ($R''/R' = 2.30 \pm 0.27$; $r_{01}/r = 1.53 \pm 0.09$; $n = 6$). Similar results held for $t_{ISI} = 100$ ms ($R''/R' = 1.95 \pm 0.22$; $r_{01}/r = 1.33 \pm 0.07$; $n = 8$) and $t_{ISI} = 250$ ms ($R''/R' = 1.64 \pm 0.19$; $r_{01}/r = 1.17 \pm 0.06$; $n = 6$; **Fig. 4d**). These data show that synaptic potency is plastic and hence that the amount of glutamate released by a single action potential can be modulated.

Can increased potency during facilitation be explained by the existence of multiple independent release sites at single active zones? If multivesicular release from several sites at the same active zone occurs, potency and release probability will change together in a predictable manner. Each active zone con-

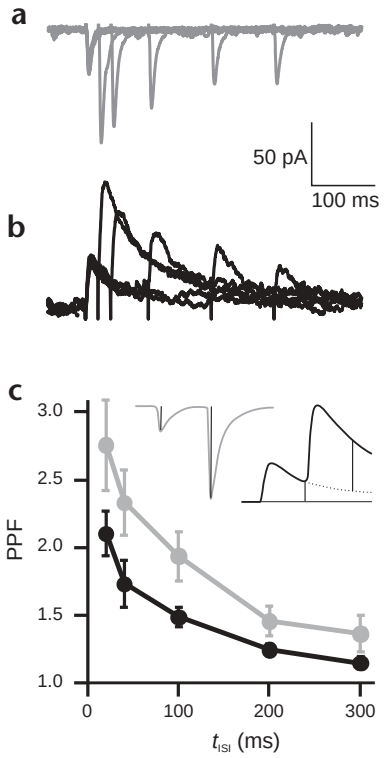

Fig. 2. Paired-pulse facilitation of excitatory postsynaptic currents. (**a**) EPSCs recorded at –70 mV for interstimulus intervals (t_{ISI}) of 20–300 ms (average of six trials). (**b**) EPSCs recorded in the same cell at +40 mV. (**c**) Paired-pulse facilitation (PPF) of EPSCs dominated by AMPAR (gray) or NMDAR (black) mediated currents. Inset, AMPAR-mediated current amplitudes were estimated as the peaks of EPSCs at –70 mV, whereas NMDAR current amplitudes were estimated 40 ms after stimulation at +40 mV. For all measurements, the response to a single stimulus was subtracted from the response to the second pulse.

tains several docked vesicles that seem poised for release (~10; equivalent to the readily releasable pool)[4]. Replenishing the readily releasable pool takes several seconds[4], and the number of docked vesicles (D) is not likely to change over the duration of a cycle in a PPF experiment unless release occurs. If each docked vesicle acts as a release site, fusing independently with probability p after an AP, then, according to the binomial model[1], the synaptic release probability in response to the first pulse is $P' = 1 - (1 - p)^D$. Owing to facilitation, after the first pulse the release probability per vesicle is enhanced by a factor α to αp ($\alpha > 1$). The release probability for the synapse on the second pulse, given that there was a failure of release to the first pulse, is then $p_{01} = 1 - (1 - \alpha p)^D$. We measured both P' and p_{01} directly (**Fig. 3b** and **c**) and used them to calculate an expected potency facilitation $(r_{01}/r)^* = (P' - P'(1-p_{01}))^{1/D})/(p_{01} - p_{01}(1-P'))^{1/D})^h$ (see equation (2), Methods). In the equation above, h is the Hill coefficient for synapses, relating NMDAR activation and the number of vesicles released (range of h, 1–1.4; see Methods). As r and r_{01} could also be measured, we compared the expected potency facilitation $(r_{01}/r)^*$ with the measured potency facilitation, r_{01}/r (**Fig. 4b**). This analysis showed that our measurements were compatible with the existence of several independent release sites per active zone and clearly inconsistent with the univesicular release rule (**Fig. 4b**). Postulating five release sites gives a satisfactory fit to the data, consistent with the number of docked vesicles reported to exist in CA1 active zones[3].

How do our single-synapse measurements of PPF_{Ca} compare to PPF averaged over multiple synapses and measured at the soma? The time courses of PPF_{Ca} and PPF were indistinguishable, suggesting that the mechanisms of plasticity are shared (**Fig. 4c** and **d**). PPF_{Ca} was larger than PPF, as probed with NMDAR-mediated currents (2.30 ± 0.27 versus 1.73 ± 0.17, t_{ISI} = 40 ms, n = 6). A quantitative comparison of facilitation amplitudes is complicated by differences in measurement techniques: different populations of synapses contribute to the responses evoked by the first and second stimulus in electrophysiological measurements, whereas the same single synapse is probed on both trials in imaging measurements.

If single active zones do contain multiple independent release sites, then pharmacological manipulation of release probability should also change synaptic potency. At CA1 hippocampal

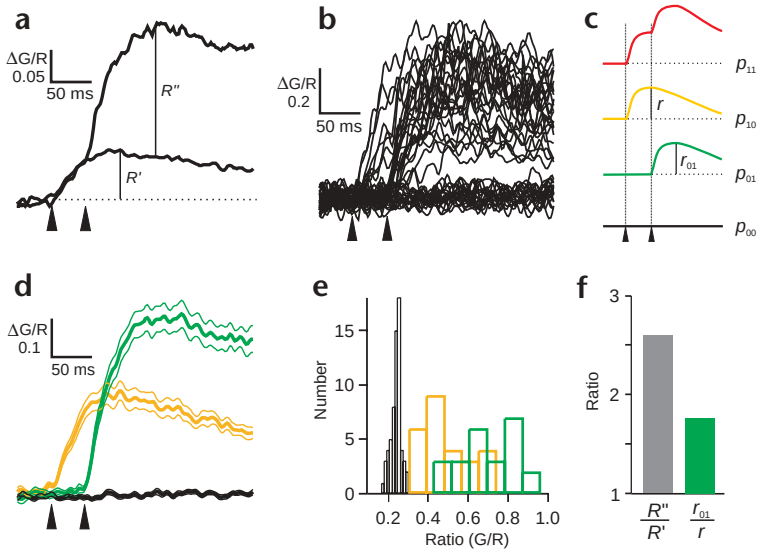

Fig. 3. Paired-pulse facilitation at a single synapse. (**a**) Average [Ca^{2+}] transient in response to a single stimulus and pair of stimuli at t_{ISI} = 40 ms. To quantify PPF_{Ca}, peak amplitudes (R' and R'') were measured as indicated by the arrows. (**b**) Responses to 45 paired-pulse stimuli. Failures of synaptic transmission can be clearly distinguished from successes. (**c**) The four possible outcomes resulting from paired-pulse stimulation with their associated probabilities (p_{11}, p_{10}, p_{01}, p_{00}). Also indicated is the potency in response to the first stimulus (r) and the potency in response to the second stimulus given that there was a failure on the first (r_{01}). (**d**) Time course of the success amplitude to a single stimulus (yellow) and to the second stimulus in a pair where the first produced a failure (green). Also shown is the failure to both stimuli (black). (**e**) Response amplitudes (yellow = r, green = r_{01}, black = failures, same data as in **d**). (**f**) Paired-pulse facilitation of the average response (gray) was in part due to facilitation in potency (green).

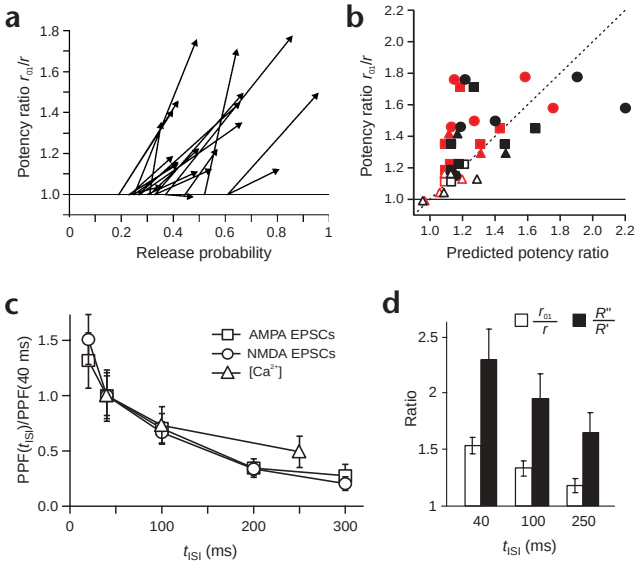

Fig. 4. Dissecting PPF in individual synapses. (**a**) Normalized potency plotted against a measure of release probability (t_{ISI} = 40 ms, n = 6; t_{ISI} = 100 ms, n = 8; t_{ISI} = 250 ms, n = 6). Arrows connect points corresponding to the control response (P', 1) with points corresponding to the facilitated response ($p_{01}/(p_{01}+p_{00})$, r_{01}/r). The x-value $p_{01}/(p_{01}+p_{00})$ is the release probability for the second stimulus given that there was a failure of release on the first. In all but one synapse, increasing release probabilities were correlated with increasing potency (arrows with positive slope). (**b**) Measured potency ratio compared to predicted potency ratio for the univesicular release rule (horizontal line) and a binomial model with five independent release sites (dotted line with slope = 1, see Methods). Black symbols show the prediction assuming a Hill coefficient h = 1, red symbols for h = 1.4. Shapes indicate different interstimulus intervals: t_{ISI} = 40 ms (circles), 100 ms (squares) and 250 ms (triangles). Filled symbols mark spines in which the measured r_{01}/r was significantly larger than 1 (Wilcoxon two-sample test, $P < 0.05$). (**c**) The time course was similar for PPF_{Ca} and PPF_i. Values are normalized to PPF at t_{ISI} = 40 ms. (**d**) Potency ratio (white bars) and total PPF_{Ca} (black bars) as a function of t_{ISI}.

synapses, activation of presynaptic A1 adenosine receptors leads to a reduction of transmitter release[30,31]. Using $[Ca^{2+}]$ imaging in individual spines, we measured the synaptic release probability, P', and potency, r. After a baseline period, we applied 2-chloroadenosine (1–5 μM), an agonist of A1 receptors. In eight of nine synapses studied, both P' and r decreased significantly, and in one synapse, 2-chloroadenosine did not induce a change in either P' or r (**Fig. 5c**, red arrows). In some experiments, washout of 2-chloroadenosine partially reversed the reduction of P', and was associated with a concomitant increase in r (**Fig. 5c**, blue arrows, n = 2). At a concentration of 20 μM, the specific A1 antagonist DPCPX caused corresponding changes in the opposite direction (**Fig. 5c**, black arrows, n = 3). The finding that P' and r consistently changed together is consistent with the existence of multiple release sites in an active zone.

Although our experiments support the idea of multiple release sites per active zone, some other mechanisms also could explain our data. As glutamate receptors are not saturated[20,24,25], any mechanism that can change the amplitude or time course of glutamate concentration in the cleft would change the occupancy of receptors and the amplitudes of postsynaptic responses. In particular, it has been suggested that glutamate release from small vesicles can occur in two modes: the classic all-or-none exocytosis and a graded mode in which glutamate diffuses through a transient fusion pore[32]. A use-dependent switch from graded mode to all-or-none mode would cause potency potentiation and could, in principle, account for our data.

A testable prediction of this model is that the glutamate transient after graded exocytosis will be smaller and longer-lasting than it is during all-or-none exocytosis[32]. This implies that the rise time of the NMDAR current would be slower[33], resulting in a slower rise of the spine $[Ca^{2+}]$ transient, which is proportional to the integral of the Ca^{2+} current under our measurement conditions[34,35]. We found, however, that the rise times of $[Ca^{2+}]$ transients in response to single stimuli were indistinguishable from those in response to the second of a pair of stimuli (**Fig. 6**). These findings indicate that under different conditions of release, char-

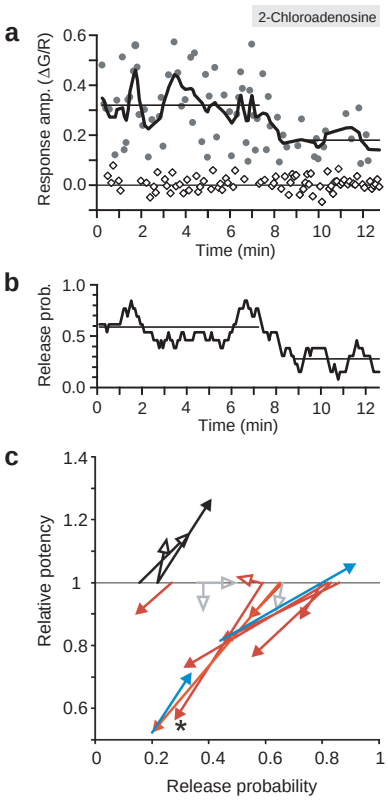

Fig. 5. Varying release probability pharmacologically changes potency. (**a**) Calcium transients from a single spine. After 7 min, 10 μM 2-Chloroadenosine was added to the bath. The size of the average success amplitude (black curve) decreased markedly (circles, successes; diamonds, failures). (**b**) Average release probability of the experiment above, calculated in an 11-point sliding window. P_r changed from 0.59 (control) to 0.28 (adenosine), indicated by the black horizontal lines. (**c**) Summary data of 13 spines in different slices treated with 2-Chloroadenosine (2–10 μM, red arrows), with 2-Chloroadenosine and subsequent washout (blue arrows) or with the A1-antagonist DPCPX (20 μM, black arrows; 5 μM, gray arrows). Filled arrowheads indicate a significant change in potency (Wilcoxon two-sample test, $P < 0.05$). The example shown in (**a**) and (**b**) is marked with an asterisk.

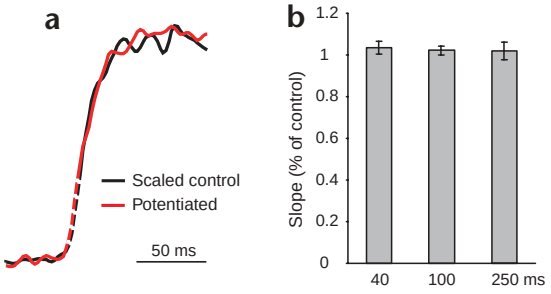

Fig. 6. Rise times of $[Ca^{2+}]$ transients under control and potentiated conditions. (**a**) Overlay of peak-normalized control (black) and potentiated (red) $[Ca^{2+}]$ transients from a single spine. The initial slope of the $[Ca^{2+}]$ transients (dashed) was used as a measure of rise time. Time course of the $[Ca^{2+}]$ transients was not changed in the potentiated responses (t_{ISI} = 40 ms, 30% potency potentiation). (**b**) Summary data for all synapses. The slopes of the potentiated responses were not different from those of controls for all interstimulus intervals (Wilcoxon matched-pair signed-rank test, n = 20).

acterized by different synaptic release probabilities, cleft glutamate transients have the same time course but different amplitudes. We conclude that fusion pore modulation is unlikely to account for our data.

Using spine Ca^{2+} accumulation as a reporter of released glutamate requires that the Ca^{2+}-sensitive dye is not saturated after the release of a single vesicle. Three lines of evidence suggest that under our experimental conditions, the fluorescence signal was approximately proportional to NMDAR activation. First, because of the large added buffer capacity for Ca^{2+} provided by the indicator, $[Ca^{2+}]$ accumulations were reduced ~30-fold compared to native conditions[35]. Based on quantitative measurements of NMDAR-mediated $[Ca^{2+}]$ accumulations, the amplitudes of these buffered transients are expected to be on the order of $\Delta[Ca^{2+}]_{syn} \approx 200–300$ nM[35], which is in the linear regime of our indicator ($\Delta[Ca^{2+}]_{syn} < K_d = 785$ nM). Second, the changes in fluorescence after depolarizing the neurons from −70 to +10 mV were ~1.7 times larger than those in response to synaptic stimuli, again indicating that synaptic $[Ca^{2+}]$ transients were far from indicator saturation. Third, in several experiments (n = 8), we explicitly tested for linearity (**Fig. 7**). If the Ca^{2+} indicator were close to saturation, larger $[Ca^{2+}]$ accumulations would have resulted in relatively compressed fluorescence responses. Consequently, our measurements of PPF_{Ca} and potency ratios (r_{01}/r) would have been underestimates of the true values. To address this issue, measurements were interleaved between holding potentials close to reversal for the NMDAR (+10 mV) and potentials closer to reversal for Ca^{2+} (+40 mV). Consistent with the changes in driving force for Ca^{2+}, responses were smaller at the higher holding potentials, r(+40 mV)/r(+10 mV) = 0.56, and were therefore expected to be more linear in the case of saturation. However, r_{01}/r was identical at both holding potentials: r_{01}/r (+10 mV) = 1.33 ± 0.07, r_{01}/r (+40 mV) = 1.26 ± 0.07 (**Fig. 7b**). We conclude that spine $[Ca^{2+}]$ is proportional to NMDAR activation.

Discussion

We imaged NMDAR-mediated $[Ca^{2+}]$ transients in single spines evoked by synaptic stimulation. As virtually all spines in the CA1 region of hippocampus form only one synapse[3,21], $[Ca^{2+}]$ imaging allowed us to measure synaptic release probability and potency (the average amplitude of the postsynaptic response to a successful synaptic transmission) at individual synapses, generating data for quantal analysis at single CA3–CA1 synapses. Using activity-dependent and pharmacological modulation of release probability, we found that potency increased with release probability. These data imply that single active zones are capable of releasing a variable amount of glutamate per action potential.

Several technical issues, however, complicate the interpretation of our experiments. Under some conditions, glutamate released from a neighboring, non-imaged synapse can diffuse to postsynaptic receptors at the imaged synapse ('spillover')[36–38] and contribute to potency facilitation ($r_{01}/r > 1$). We consider this mechanism unlikely because we used stimuli that activate only a tiny subpopulation of synapses (<5%), implying that the probability of activating multiple varicosities within diffusion distance was small[36]. Studies specifically designed to detect correlations in the response amplitudes of neighboring spines do not show evidence of spillover[20] (E. A. N. & K. S., *Soc. Neurosci. Abstr.* **27**, 155.2, 2001). Consistent with this finding, published evidence for spillover was collected primarily at low temperatures[38] or in the presence of blockers of astrocytic glutamate transporters[36,37], not under our experimental conditions. Furthermore, in our experiments, double-failure trials (r_{00}) were indistinguishable from baseline (**Fig. 3d**), inconsistent with spillover from other active synapses that were not imaged.

Even spillover too weak to activate NMDARs, however, could leave its mark by producing receptors singly bound by glutamate. This glutamate would sum with direct release of glutamate to potentiate NMDAR activation. For two reasons, this spillover model cannot account for our data. First, the potency facilitation produced in this situation is, at most, $1 + 2\Delta P_d\alpha$, where ΔP_d is the change in the release probability of the non-imaged ('dark') synapse, and α is the fraction of glutamate escaping to a neighboring synapse (see Methods for derivation). Even assuming a large α = 0.1 (refs. 39 and 40), one would expect potency facilitation in the range of 0–15%, which is much smaller than what we measured (0–80%, **Fig. 4b**). Second, in the spillover model, potency facilitation is expected to be independent of release probability and PPF at the imaged synapse (equation (3), Methods). This is inconsistent with the correlation between measured potency ratio and predicted potency ratio (a function of release probabilities at the imaged synapse, **Fig. 4b**). Thus, spillover and

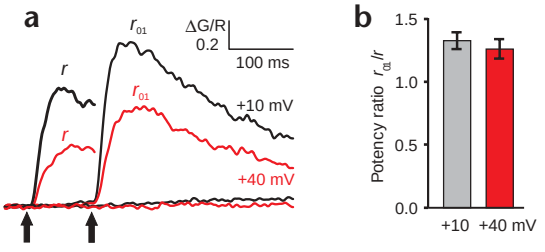

Fig. 7. Change in potency is constant as a function of holding potential. (**a**) Average success to the first stimulus (r), average success to the second stimulus given a failure to the first (r_{01}) and average failure at +10 mV (black curves) and at +40 mV (red curves) for a single synapse. Trials at different holding potentials were interleaved, t_{ISI} = 100 ms. (**b**) Summary data for eight synapses showing that the potency ratio was the same at both holding potentials and significantly ($P < 0.01$) larger than 1.

pooling of glutamate can only account for a small fraction of the potency facilitation we observed.

Release of Ca^{2+} from intracellular stores could also contribute to postsynaptic $[Ca^{2+}]$ signals under certain conditions[41] and confound our interpretation of spine $[Ca^{2+}]$ as a measure of NMDAR activation. However, three lines of evidence argue against this possibility. First, release from stores has not been observed under experimental conditions that are similar to ours[20,42]. Second, most spines do not contain endoplasmic reticulum (ER)[43], so release from stores would most likely be initiated in the dendritic shaft, but in our experiments spines were activated without concomitant dendritic $[Ca^{2+}]$ signals (**Fig. 1a** and **b**). Third, $[Ca^{2+}]$ accumulations varied with holding potential as expected for Ca^{2+} influx through NMDARs (**Fig. 7**). These observations led us to conclude that intracellular stores did not contribute to the $[Ca^{2+}]$ signal.

At CA3–CA1 synapses, successful glutamate release in response to low-frequency stimulation opens only a few NMDAR receptors on average (2–5 receptors, unpub. observ.). Therefore, failures of postsynaptic $[Ca^{2+}]$ transients could, in rare instances, be due to receptor failures after transmitter release. On arrival of the second pulse, some NMDA receptors could still be singly bound by glutamate without opening[33,44]. An upper bound on the potency facilitation that could be caused by this mechanism can be estimated as 3.3% for a 40-ms ISI, 2.5% for a 100-ms ISI, and 1% for a 250-ms ISI—not sufficient to account for our data. Furthermore, experiments using pharmacological manipulations of release probability (**Fig. 5**) were not affected by the possibility of receptor failures.

Our results indicate that, at higher release probabilities, more glutamate is released per action potential. As neurotransmitter is released in quanta corresponding to individual vesicles, and as single active zones contain multiple docked vesicles, the most parsimonious explanation of our data is that multiple vesicles can be released in response to a single AP and the probability of multivesicular release increases with synaptic release probability. The monotonic relationship between release probability and potency that we found (**Figs. 4b** and **5c**) is in quantitative agreement with a binomial model that includes several independent release sites. We suggest that these release sites correspond to the docked vesicles that are seen under the electron microscope[2].

Some studies show, using minimal stimulation, that potency remains unchanged under conditions that modulate release, consistent with the univesicular release rule[5,10]. Differences between these studies and our imaging experiments may be due to differences in preparation (neonatal versus juvenile slice) or to experimental conditions (room temperature versus 34°C). Another possibility is that different methods (electrophysiology versus imaging) select for different types of synapses. For example, our measurements probably excluded the smallest spines, presumably corresponding to the smallest synapses. Owing to the strong dendritic filtering of currents arising from distant synapses[8,18], failure analysis using somatic patch-clamp recordings probably selects for large synapses close to the soma. Resolving the discrepancy between these electrophysiological measurements and our optical measurements will require further studies that perhaps apply both types of analysis to the same synapse.

According to the binomial model, if the release probability (P_r) of a small synapse is low, most successful transmissions will be due to the release of a single vesicle (for example, 92% of releases are single-vesicle releases for a synapse with five release sites and $P_r = 0.2$). As P_r rises, the fraction of multivesicular events increases: for the same synapse at $P = 0.6$, 67% of releases are univesicular and 33% are multivesicular. The finding that the spine Ca^{2+} transients reflect the predicted changes in cleft glutamate concentration confirms that NMDA receptors are far from saturation after the release of a single vesicle[20]. At each synapse, the coupling between changes in synaptic release probability and potency will result in larger unitary synaptic currents during high-frequency stimulation (bursts) and smaller unitary currents in response to isolated APs. The potentiated Ca^{2+} accumulations observed during facilitation (**Fig. 3d**) may selectively trigger some kinds of use-dependent postsynaptic plasticity[45]. The possibility of multivesicular release implies that even synapses with reliable responses to a single AP (high synaptic release probability) could still increase the number of released vesicles per AP, thus expanding the effective dynamic range for facilitation. Finally, it is possible that univesicular release at some synapses predominantly activates NMDARs and multivesicular release at other synapses activates lower-affinity AMPARs. This is another possible presynaptic explanation[32,46] for a subset of silent synapses[47,48].

Methods

Preparation and electrophysiology. Horizontal hippocampal slices (350 μm thick) were prepared from Wistar rats 16–19 days old in accordance with the animal care and use guidelines of Cold Spring Harbor Laboratory, using a chilled cutting solution containing 110 mM choline chloride, 25 mM $NaHCO_3$, 25 mM D-glucose, 11.6 mM sodium ascorbate, 7 mM $MgSO_4$, 3.1 mM sodium pyruvate, 2.5 mM KCl, 1.25 mM NaH_2PO_4 and 0.5 mM $CaCl_2$. Slices were incubated in gassed (95% O_2 and 5% CO_2) physiological saline (127 mM NaCl, 25 mM $NaHCO_3$, 25 mM D-glucose, 2.5 mM KCl, 1.5 mM $MgCl_2$, 1.5 mM $CaCl_2$ and 1.25 mM NaH_2PO_4) at 34°C for 30–45 min and then at room temperature until used. Experiments were done at 34°C in physiological saline containing 0.01 mM NBQX, 0.01 mM bicuculline and 0.01 mM serine (Sigma, St. Louis, Missouri). Whole-cell patch electrodes (3–6 MΩ) contained 135 mM $CsMeSO_3$, 10 mM HEPES, 10 mM sodium phosphocreatine, 5 mM glutathione, 4 mM $MgCl_2$, 4 mM Na_2-ATP, 0.4 mM Na-GTP, 0.6 mM Fluo5F and 0.04 mM Alexa Fluor 594 (Molecular Probes, Eugene, Oregon). Cells were depolarized to +10 mV to relieve the Mg^{2+} block of NMDARs and to inactivate voltage-sensitive Ca^{2+} channels. Synaptic transmission was evoked by short current pulses delivered with a glass pipette (2–3 μm tip)[20]. Paired pulses and single pulses were alternated every five seconds.

Two-photon imaging. We used a custom built two-photon laser scanning microscope[49] consisting of a Ti:sapphire laser (Mira, Coherent, Santa Clara, California) tuned to λ ~810 nm, a 63× 0.9NA Objective (Olympus, Melville, New York) and a Zeiss scan lens (Zeiss, Thornwood, New York). Fluorescence was detected in epifluorescence and transfluorescence (through an oil-immersion condenser, Zeiss, NA = 1.4) modes using photomultiplier tubes (R3896, Hamamatsu, Hamamatsu City, Japan). Image acquisition was controlled by custom software written in Matlab (MathWorks, Natick, Massachusetts). In the transfluorescence pathway, a 565-nm dichroic mirror was used to separate green and red fluorescence. BG22-colored glass filters and 607/45 barrier filters were placed respectively in the 'green' (shorter wavelength) and 'red' (longer wavelength) pathways to eliminate transmitted or reflected excitation light. (All filters and dichroic mirrors were from Chroma, Battleboro, Vermont.) Neurons were filled through the patch electrode for more than 15 min before imaging. To measure a fluorescence signal proportional to $[Ca^{2+}]$, we used large concentrations (600 μM) of a medium-affinity (K_d = 785 nM under physiological conditions, data not shown) Ca^{2+} indicator, Fluo5F (Molecular Probes), detected as green fluorescence. Fluo5F is too dim at rest to reliably image spines, so we added a Ca^{2+}-insensitive fluorophore (Alexa Fluor 594) to the pipette solution, detected in the red channel (**Fig. 1 a–c**). Stimulated synapses on higher-order apical dendrites (70–380 μm from the soma) were identified in frame scans with

an on-line analysis program written in IGOR (Wavemetrics, Lake Oswego, Oregon) (**Fig. 1a**). In the paired-pulse experiments, the activated spine was centered in a 15 × 15 μm window and probed using line scans with a temporal resolution of 2 ms (**Fig. 1b**). In the pharmacological experiments, where high temporal resolution was not a requirement, four frame scans (64 × 64 pixel) were acquired in each trial (two before and two after the stimulus). Only synapses in which stable responses from well-isolated Ca^{2+} sources could be verified were analyzed. Spine volumes were in the range from 0.032 to 0.183 μm^3, mean volume 0.081 μm^3 ($n = 21$, collected in a separate set of experiments using identical selection criteria).

Data analysis. As the resting fluorescence of Fluo5F is very low, calculating $\Delta F/F$ introduces large errors due to shot noise. Thus we used the ratio of green:red fluorescence intensity, $\Delta G/R$; this measure is independent of absolute dye concentration and robust to movement artifacts. To avoid problems with background subtraction, care was taken to avoid ejecting dye from the pipette into the slice[35]. Cells in which the surrounding slice showed detectable background fluorescence after dye loading were not used. The only background correction that was done was subtraction of the photomultiplier tube dark current. The threshold for detection of successes was set individually for each spine in a plot of all individual trials from that spine (**Fig. 3b**). Only spines that showed a clear separation between failures and successes were included in the analysis. The sorting threshold was set in the middle of the gap between failure and success trials. First, successes to the first stimulus (r_1, which may have failed or succeeded to the second stimulus) were detected, removed from the plot, and averaged separately. Second, successes to the second stimulus (r_{01}) were separated from complete failures of transmission (r_{00}) and averaged separately (**Fig. 3d**). Tests of significance used the Wilcoxon two-sample test unless otherwise noted. All measurements are given as mean ± s.e.m.

Quantal analysis of short-term synaptic plasticity. The number of successes divided by the number of trials is the probability of release for a synapse, P', in response to a single pulse (or the first pulse in a pair). Let γ be the fluorescence signal produced by the release of a single vesicle. The success amplitude to a single stimulus is the potency $r = \gamma n^h$, where n is the average number of vesicles released on success trials only and h is the effective Hill coefficient, describing the response of synaptic receptors as a function of the number of vesicles released. If glutamate released from different vesicles interacts with distinct subsets of receptors, then $h = 1$. If glutamate from different vesicles interact with the same population of receptors, then $h = 1.4$, the Hill coefficient for the concentration–response curves for NMDARs[50].

In a paired-pulse experiment, responses were sorted into (i) complete failures of transmission (with probability p_{00}), (ii) responses to the second stimulus only (p_{01}) and (iii) responses to the first stimulus and either failure (p_{10}) or success (p_{11}) to the second stimulus. Then the average fluorescence response to the first pulse, including failures, is $R' = (p_{11} + p_{10})r$. In general, in response to a pair of stimuli, the potency of the second pulse may vary depending on whether there was release on the first pulse. We denote as r_{11} and r_{01} the potencies of the second pulse given that release did (r_{11}) or did not (r_{01}) occur on the first pulse. The average response to the second pulse in a pair is then $R'' = p_{11}r_{11} + p_{01}r_{01}$. The PPF is the average response to the second pulse relative to the average response to the first pulse, $\mathrm{PPF} = R''/R' = (p_{11}r_{11} + p_{01}r_{01})/(p_{11} + p_{10})r$. In the special case where at most one vesicle can be released per AP (univesicular release rule), $r = r_{01} = r_{11}$, and PPF is simply equal to the relative change in release probability on the second and first pulse: $\mathrm{PPF} = P''/P' = (p_{01} - p_{10})/(p_{11} + p_{10})$.

Models of short-term synaptic plasticity at single synapses. We compared the number of vesicles released by successes on pulse one (n) and pulse two, under the condition that there was no release on the first pulse (n_{01}). These are related to potencies as $r = \gamma n^h$ and $r_{01} = \gamma n_{01}{}^h$. The potencies can be measured (**Fig. 3**) together with their associated release probabilities P' and p_{01}, respectively. In a simple model of release, an active zone contains D docked vesicles where each vesicle can release independently with a release probability p. Thus, each docked vesicle serves as an independent release site. Conditions of PPF increase the vesicle release probability to αp, where $\alpha > 1$. The number of vesicles released by successes is then as follows:

$$n = \frac{pD}{P'} \text{ and } n_{01} = \frac{\alpha pD}{p_{01}}$$

This yields the following ratio:

$$\frac{n_{01}}{n} = \frac{P'}{p_{01}}\alpha \tag{1}$$

According to the binomial model, the release probabilities are $P' = 1 - (1-p)^D$ and $p_{01} = 1 - (1-\alpha p)^D$. We can compute the number of released vesicles by solving these expressions for α in terms of measurable quantities and inserting into equation (1):

$$\frac{n_{01}}{n} = \frac{P' - P'(1-p_{01})^{1/D}}{p_{01} - p_{01}(1-P')^{1/D}} \tag{2}$$

To relate the potencies to the ratio of vesicles released, we use the following relationship:

$$\frac{r_{01}}{r} = \left(\frac{n_{01}}{n}\right)^h$$

Potency facilitation due to spillover. Could spillover explain the potency facilitation we observed (**Fig. 4b**)? We considered the situation when spillover occurs between two nearby synapses: the 'imaged' synapse (i) and the non-imaged 'dark' synapse (d). Spillover is characterized by the parameter α, the fraction of glutamate released at one synapse that reaches a neighboring synapse. In previous measurements, we saw clear and complete transmission failures, and no response correlations between neighboring spines[20] (E. A. N. & K. S., *Soc. Neurosci. Abstr.*, **27**, 155.2, 2001), so we assumed that spillover of glutamate alone is not sufficient to produce NMDAR activation, but rather produces a population of singly bound receptors. Spillover of glutamate combines, however, with directly released glutamate to produce potency facilitation. Seeking to derive a worst-case scenario, we used a Hill coefficient of 2. Then the potency at the imaged synapse, to first order in α, is the following:

$$r \approx \gamma c^2(1 + 2P_d\alpha)$$

Here, c is an effective concentration of glutamate in the cleft, and γ is a constant. Note that r is independent of the release probability at the imaged synapse, P_i. The potency facilitation follows:

$$\frac{r_{01}}{r} \approx (1 + 2(P_d'' - P_d')\alpha) \tag{3}$$

Acknowledgments

We thank Z. Mainen, R. Malinow, M. Maravall and R. Yasuda for comments on the manuscript, and T. Pologruto for software development. This work was supported by grants from the Swartz Initiative for Computational Neuroscience (to T.G.O.), the Helen Hay Whitney Foundation (to B.L.S.), the Pew and Mathers Foundations and the National Institutes of Health (NIH).

Competing interests statement

The authors declare that they have no competing financial interests.

RECEIVED 18 MARCH; ACCEPTED 8 MAY 2002

1. Katz, B. *The Release of Neural Transmitter Substances* (Thomas, Springfield, Illinois, 1969).
2. Harris, K. M. & Sultan, P. Variation in the number, location and size of synaptic vesicles provides an anatomical basis for the nonuniform probability

of release at hippocampal CA1 synapses. *Neuropharmacology* **34**, 1387–1395 (1995).
3. Schikorski, T. & Stevens, C. F. Quantitative ultrastructural analysis of hippocampal excitatory synapses. *J. Neurosci.* **17**, 5858–5867 (1997).
4. Dobrunz, L. E. & Stevens, C. F. Heterogeneity of release probability, facilitation, and depletion at central synapses. *Neuron* **18**, 995–1008 (1997).
5. Hanse, E. & Gustafsson, B. Quantal variability at glutamatergic synapses in area CA1 of the rat neonatal hippocampus. *J. Physiol.* **531**, 467–480 (2001).
6. Auger, C., Kondo, S. & Marty, A. Multivesicular release at single functional synaptic sites in cerebellar stellate and basket cells. *J. Neurosci.* **18**, 4532–4547 (1998).
7. Tong, G. & Jahr, C. E. Multivesicular release from excitatory synapses of cultured hippocampal neurons. *Neuron* **12**, 51–59 (1994).
8. Isaac, J. T. *et al.* An investigation of the expression mechanism of LTP of AMPA receptor–mediated synaptic transmission at hippocampal CA1 synapses using failures analysis and dendritic recordings. *Neuropharmacology* **37**, 1399–1410 (1998).
9. Wadiche, J. I. & Jahr, C. E. Multivesicular release at climbing fiber-purkinje cell synapses. *Neuron* **32**, 301–313 (2001).
10. Stevens, C. F. & Wang, Y. Facilitation and depression at single central synapses. *Neuron* **14**, 795–802 (1995).
11. Redman, S. Quantal analysis of synaptic potentials in neurons of the central nervous system. *Physiol. Rev.* **70**, 165–198 (1990).
12. Regehr, W. G. & Stevens, C. F. in *Synapses* (eds. Cowan, W. M., Sudhof, T. C. & Stevens, C. F.) 135–175 (Johns Hopkins Univ. Press, Baltimore, 2001).
13. Auger, C. & Marty, A. Quantal currents at single-site central synapses. *J. Physiol.* **526**, 3–11 (2000).
14. Korn, H., Triller, A., Mallet, A. & Faber, D. S. Fluctuating responses at a central synapse: *n* of binomial fit predicts number of stained presynaptic boutons. *Science* **213**, 898–901 (1981).
15. Spruston, N., Jonas, P. & Sakmann, B. Dendritic glutamate receptor channels in rat hippocampal CA3 and CA1 pyramidal neurons. *J. Physiol.* **482**, 325–352 (1995).
16. Faber, D. S., Young, W. S., Legendre, P. & Korn, H. Intrinsic quantal variability due to stochastic properties of receptor–transmitter interactions. *Science* **258**, 1494–1498 (1992).
17. Magee, J. C. & Cook, E. P. Somatic EPSP amplitude is independent of synapse location in hippocampal pyramidal neurons. *Nat. Neurosci.* **3**, 895–903 (2000).
18. Stuart, G. & Spruston, N. Determinants of voltage attenuation in neocortical pyramidal neuron dendrites. *J. Neurosci.* **18**, 3501–3510 (1998).
19. Williams, S. R. & Stuart, G. J. Dependence of EPSP efficacy on synapse location in neocortical pyramidal neurons. *Science* **295**, 1907–1910 (2002).
20. Mainen, Z. F., Malinow, R. & Svoboda, K. Synaptic calcium transients in single spines indicate that NMDA receptors are not saturated. *Nature* **399**, 151–155 (1999).
21. Harris, K. M. & Stevens, J. K. Dendritic spines of CA1 pyramidal cells in the rat hippocampus: serial electron microscopy with reference to their biophysical characteristics. *J. Neurosci.* **9**, 2982–2997 (1989).
22. Yuste, R. & Denk, W. Dendritic spines as basic functional units of neuronal integration. *Nature* **375**, 682–684 (1995).
23. Denk, W. & Svoboda, K. Photon upmanship: why multiphoton imaging is more than a gimmick. *Neuron* **18**, 351–357 (1997).
24. McAllister, A. K. & Stevens, C. F. Nonsaturation of AMPA and NMDA receptors at hippocampal synapses. *Proc. Natl. Acad. Sci. USA* **97**, 6173–6178 (2000).
25. Umemiya, M., Senda, M. & Murphy, T. H. Behavior of NMDA and AMPA receptor-mediated miniature EPSCs at rat cortical neuron synapses identified by calcium imaging. *J. Physiol.* **521**, 113–122 (1999).
26. Sabatini, B. L., Maravall, M. & Svoboda, K. Ca^{2+} signaling in dendritic spines. *Curr. Opin. Neurobiol.* **11**, 349–356 (2001).
27. Mainen, Z. F. *et al.* Two-photon imaging in living brain slices. *Methods* **18**, 231–239 (1999).
28. Bekkers, J. M., Richerson, G. B. & Stevens, C. F. Origins of variability in quantal size in cultured hippocampal neurons and hippocampal slices. *Proc. Natl. Acad. Sci. USA* **87**, 5359–5362 (1990).
29. Zucker, R. S. & Regehr, W. G. Short-term synaptic plasticity. *Annu. Rev. Neurosci.* **12**, 13–31 (1989).
30. Wu, L. G. & Saggau, P. Adenosine inhibits evoked synaptic transmission primarily by reducing presynaptic calcium influx in area CA1 of hippocampus. *Neuron* **12**, 1139–1148 (1994).
31. Wu, L. G. & Saggau, P. Presynaptic inhibition of elicited neurotransmitter release. *Trends Neurosci.* **20**, 204–212 (1997).
32. Choi, S., Klingauf, J. & Tsien, R. W. Postfusional regulation of cleft glutamate concentration during LTP at 'silent synapses.' *Nat. Neurosci.* **3**, 330–336 (2000).
33. Clements, J. D. & Westbrook, G. L. Activation kinetics reveal the number of glutamate and glycine binding sites on the *N*-methyl-D-aspartate receptor. *Neuron* **7**, 605–613 (1991).
34. Neher, E. The use of Fura-2 for estimating Ca buffers and Ca fluxes. *Neuropharmacology* **34**, 1423–1442 (1995).
35. Sabatini, B. S., Oertner, T. G. & Svoboda, K. The life-cycle of Ca^{2+} ions in spines. *Neuron* **33**, 439–452 (2002).
36. Asztely, F., Erdemli, G. & Kullmann, D. M. Extrasynaptic glutamate spillover in the hippocampus: dependence on temperature and the role of active glutamate uptake. *Neuron* **18**, 281–293 (1997).
37. Arnth-Jensen, N., Jabaudon, D. & Scanziani, M. Cooperation between independent hippocampal synapses is controlled by glutamate uptake. *Nat. Neurosci.* **5**, 325–331 (2002).
38. Diamond, J. S. Neuronal glutamate transporters limit activation of NMDA receptors by neurotransmitter spillover on CA1 pyramidal cells. *J. Neurosci.* **21**, 8328–8338 (2001).
39. Barbour, B. An evaluation of synapse independence. *J. Neurosci.* **21**, 7969–7984 (2001).
40. Rusakov, D. A. & Kullmann, D. M. Extrasynaptic glutamate diffusion in the hippocampus: ultrastructural constraints, uptake, and receptor activation. *J. Neurosci.* **18**, 3158–3170 (1998).
41. Emptage, N., Bliss, T. V. P. & Fine, A. Single synaptic events evoke NMDA receptor-mediated release of calcium from internal stores in hippocampal dendritic spines. *Neuron* **22**, 115–124 (1999).
42. Kovalchuk, Y., Eilers, J., Lisman, J. & Konnerth, A. NMDA receptor–mediated subthreshold Ca^{2+} signals in spines of hippocampal neurons. *J. Neurosci.* **20**, 1791–1799 (2000).
43. Spacek, J. & Harris, K. M. Three-dimensional organization of smooth endoplasmic reticulum in hippocampal CA1 dendrites and dendritic spines of the immature and mature rat. *J. Neurosci.* **17**, 190–203 (1997).
44. Patneau, D. K. & Mayer, M. L. Structure–activity relationships for amino acid transmitter candidates acting at *N*-methyl-D-aspartate and quisqualate receptors. *J. Neurosci.* **10**, 2385–2399 (1990).
45. Bliss, T. V. P. & Collingridge, G. L. A synaptic model of memory: long-term potentiation in the hippocampus. *Nature* **361**, 31–39 (1993).
46. Renger, J. J., Egles, C. & Liu, G. A developmental switch in neurotransmitter flux enhances synaptic efficacy by affecting AMPA receptor activation. *Neuron* **29**, 469–484 (2001).
47. Liao, D., Hessler, N. A. & Malinow, R. Activation of postsynaptically silent synapses during pairing-induced LTP in CA1 region of hippocampal slice. *Nature* **375**, 400–404 (1995).
48. Isaac, J. T., Nicoll, R. A. & Malenka, R. C. Evidence for silent synapses: implications for the expression of LTP. *Neuron* **15**, 427–434 (1995).
49. Sabatini, B. L. & Svoboda, K. Analsyis of calcium channels in single spines using optical fluctuation analysis. *Nature* **408**, 589–593 (2000).
50. Sather, W., Dieudonne, S., MacDonald, J. F. & Ascher, P. Activation and desensitization of *N*-methyl-D-aspartate receptors in nucleated outside-out patches from mouse neurons. *J. Physiol.* **450**, 643–672 (1992).